Sensors and Materials, Vol. 37, No. 1 (2025) 359–368
MYU Tokyo

S & M 3913

Performance Enhancement of Chlorine-doped ZnO Nanorod as Piezoelectric Nanogenerators

Yu-Chi Lin,[1] Tung-Lung Wu,[2] Kao-Wei Min,[3*] Ying-Tong Ye,[4] Ming-Ta Yu,[5] Chi-Ting Ho,[5] and Teen-Hang Meen[4**]

[1]College of Engineering, National Formosa University, Huwei, Yunlin 632, Taiwan
[2]Department of Electrical Engineering, Lunghwa University of Science and Technology, Guishan District, Taoyuan City 333, Taiwan
[3]Department of Electronic Engineering, Lunghwa University of Science and Technology, Guishan District, Taoyuan City 333, Taiwan
[4]Department of Electronic Engineering, National Formosa University, Huwei, Yunlin 632, Taiwan
[5]Department of Mechanical Design Engineering, National Formosa University, Huwei, Yunlin 632, Taiwan

(Received August 5, 2024; accepted December 27, 2024)

Keywords: piezoelectric nanogenerators, sodium chloride, zinc oxide nanorod arrays, hydrothermal method

Zinc oxide (ZnO) is considered a highly promising photovoltaic material due to its low resistivity and high transmittance properties. Modifying the surface chemical properties of semiconductors by doping chemicals is an effective method of enhancing their performance. Recently, a piezoelectric nanogenerator (PENG) has been used for sustainable energy production as a promising solution. To improve the output performance of PENG, we doped ZnO nanorod arrays with chlorine in this study. To grow low-density chlorine-doped ZnO nanorod structures on indium tin oxide glass without a seed layer, we employed a hydrothermal method. These structures were then used to fabricate nanogenerators. The differences between substrates with and without seed layers were compared in terms of nanorod growth and the impact of doping the nanorods. After sputtering a layer of platinum (Pt) film onto the ZnO nanorod arrays, nanogenerators were assembled to have sputtered and nonsputtered nanostructures at the same time. These chlorine-dopped nanogenerators were driven by ultrasound to measure the optimal current–voltage (I–V) characteristics, and the results showed a current of 5.62×10^{-6} A and a voltage of 4.17×10^{-2} V, indicating a significant performance improvement. Applications of the chlorine-doped ZnO nanorod arrays are substantial as they can be used in energy harvesting devices that are adopted in self-powered systems. The arrays also are used to advance nanotechnology in energy solutions.

1. Introduction

The threats posed by global warming and the energy crisis to humanity have become increasingly severe recently. To address these issues, scientists have been finding various green

*Corresponding author: e-mail: x56784834@gmail.com
**Corresponding author: e-mail: thmeen@gs.nfu.edu.tw
https://doi.org/10.18494/SAM5275

ISSN 0914-4935
https://myukk.org/

renewable energy sources. Besides the well-known solar, wind, hydro, biomass, marine, and geothermal energy devices, smaller energy devices have been developed by many researchers. These smaller energy devices are used for implantable biosensors, chemical and biomolecular sensors, microelectromechanical systems (MEMS), remote environmental sensors, nanorobots, and wearable personal electronic products as they require durable, long-lasting, low-maintenance, and continuously operating energy generators or storage devices.

The development of such energy devices has become more urgent than before because of the need to provide sustainable power and reduce reliance on nonrenewable energy sources. By improving the efficiency and reliability of energy storage and generation at the micro- and nanoscales, innovations in medical technology, environmental monitoring, and personal electronics can be realized, ultimately enhancing the quality of life and promoting environmental sustainability.[1,2] Hence, the development of nanotechnology to convert naturally occurring mechanical energy (such as flow, motion, sound waves, or vibrations) into electrical energy is imperative. This technology enables the development of nanodevices that do not require an external power source. The self-generating properties ensure that such nanodevices are always ready to operate. Therefore, self-powering systems hold significant research significance in various applications.

With the rapid development of nanotechnology, nanoscale components require self-generated power. Although conventional batteries can power the components, they inevitably must be replaced when their power is depleted. Devices such as medical equipment inside the human body, implantable biosensors, mobile environmental sensors, and nanorobots must be standalone, free of maintenance, and self-sustainable. Such devices demand nanogenerators to serve as power sources.[3–5] Since they provide efficient, reliable, and continuous power ranging from microwatts to milliwatts, nanogenerators meet the needs of various nanoscale devices.

Nanogenerators are categorized into piezoelectric nanogenerators (PENGs)[6,7] and triboelectric nanogenerators (TENGs). In this study, we studied a nanogenerator with ZnO nanowire arrays that converts mechanical energy into electrical energy via the piezoelectric effect. The nanogenerator generates piezoelectric potential in the nanowires under external pressure. The mechanical deformation of the nanowires induces a transient flow of electrons in the external load circuit to generate the piezoelectric potential. These nanowires can generate power even by weak vibrations. The trigger frequencies range from one to several thousand hertz (Hz). This makes them highly appropriate for harvesting energy.

Recent research has shown that zinc oxide (ZnO) exhibits the characteristics of one-dimensional (1-D) nanomaterials.[8,9] To prepare ZnO nanorods, gas-phase and liquid-phase methods are used. In the gas-phase method, high-temperature-furnace chemical vapor deposition, pulse-laser deposition, and metal-organic chemical vapor deposition are conducted. In the liquid-phase method, electrophoresis,[10] the template method,[11] and the hydrothermal method are used.[8,9] In this study, we utilized the hydrothermal method to grow ZnO nanorods as the method offers advantages such as low cost, simplicity of fabrication, low defect formation, and high success rate compared with other methods. Different fabrication methods are used to make different nanostructures. One-dimensional ZnO nanostructures serve not only as the foundation for theoretical research on, for example, optical, electrical, magnetic, and mechanical

properties but also allow for nanophotonic devices to have great potential due to their optoelectronic properties. As ZnO is a piezoelectric semiconductor, when prepared in 1-D form, it can be a nanogenerator component.

By varying the concentration of doped chlorine to modify ZnO nanorods, we revealed that ZnO nanorods doped with chlorine produce a significantly higher electrical output than pure ZnO nanorods in this study. We grew ZnO nanorod arrays on an indium tin oxide (ITO) substrate with a ZnO seed layer and a self-assembled monolayer of molecules (SAMM). Enhancement in the performance of the piezoelectric nanogenerators highlights the potential of chlorine doping of ZnO nanorods to improve the generation of energy and the efficiency of nanodevices. It was also found that SAMM enhances the efficiency of the fabricated nanogenerator.

2. Material Preparation

The substrate for ZnO nanomaterials was ITO transparent conductive glass. This glass had an area of 37 × 40 cm^2, a sheet resistance of less than 10 Ω/sq, and a thickness of 0.7 mm, and was cut into pieces of 1.5 × 3 cm^2 using a glass cutter. The substrate was cleaned thoroughly before film adhesion. The thickness of the film was 1800 Å The cleaned ITO conductive glass was placed in an autoclave with a small vial containing 0.2 mL of octadecyltrichlorosilane and then heated in an oven at 150 °C for 60 min. This thermal vapor deposition process was used to form SAMM on the substrate surface. The hydrophobicity and hydrophilicity of the film were measured using a contact angle measurement method. In this study, the solution employed for growing chlorine-doped ZnO nanorod arrays consisted of hexamethylenetetramine (HMTA), zinc nitrate hexahydrate [$Zn(NO_3)_2$], and sodium chloride (NaCl) in a 1:1:x mole ratio, where x was varied from 0 to 0.4. The growth process was conducted by hydrothermal synthesis for 12 h at 95 °C.

After preparing the materials, the coated counter electrode was assembled with the ZnO nanorods (in Fig. 1). The detailed assembly process is as follows.

(1) Silver wires were connected to the ends of the counter electrode and ZnO nanorod samples using copper tape.
(2) The two samples were placed with their surfaces overlapping within a laminating film.
(3) The assembly was encapsulated on a heating platform.

The optical adhesive was used to fill gaps for waterproofing. The assembled device is shown in Fig. 2.

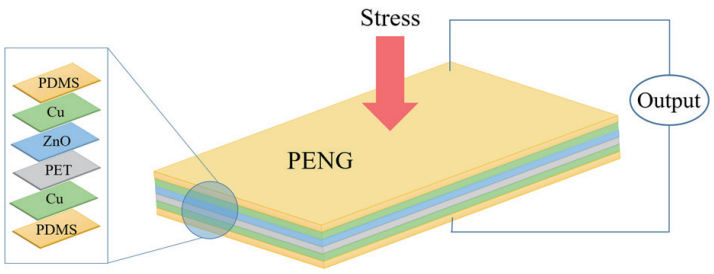

Fig. 1. (Color online) Schematic diagram of piezoelectric nanogenerator.

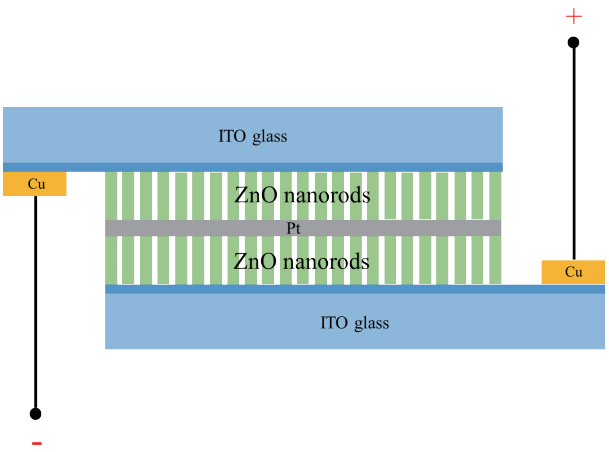

Fig. 2. (Color online) Schematic diagram of nanogenerator component.

3. Results and Discussion

When metal comes into contact with a semiconductor, Schottky and ohmic contacts are observed. Ohmic contact occurs when there is no potential difference at the junction between the metal and the semiconductor, resulting in the symmetrical conductivity of electrons under forward or reverse bias. In this case, the current–voltage curve is linear, as shown in Fig. 3. If there is a potential difference at the junction, the electron transfer at the junction becomes unsymmetrical, resulting in Schottky contact with a current–voltage curve as depicted in Fig. 3.

Figures 4(a) and 4(b) show the contact angles of the ITO glass and untreated glass substrate, respectively. The contact angle of a water droplet on the surface of the glass substrate changed from 46.58 to 81.71°. A contact angle change of 35.13° is larger than that on the untreated glass substrate (self-assembled monolayer). The base width decreased by 0.56°. This indicates that the silane molecules have successfully bonded to the ITO glass substrate, forming a hydrophobic film.

The top view of the image taken by field emission scanning electron microscopy (FE-SEM) showed that the ZnO film was uniformly and smoothly deposited on the surface of the ITO glass substrate. The side view revealed that the ZnO film adhered well to the ITO glass substrate. The nanorods grown on the ZnO seed film were denser than those grown on the untreated glass substrate. The density was increased as the ZnO film acts as a “seed layer” and facilitates the growth of ZnO nanorods to make it easier for ZnO nanoparticles to adhere to the substrate. The cross-sectional view of the nanorods grown on the ZnO seed film illustrated that the nanorods grew vertically from the substrate with a column height of 2.2 μm. The cross-sectional view shows the nanorods grown on self-assembled monolayers with a column height of 9.4 μm. The absence of the ZnO film seed layer resulted in fewer nanorods, thereby increasing their height. Without the stabilizing effect of the ZnO film, the nanorods near the fracture edges tend to tilt easily when subjected to external forces.

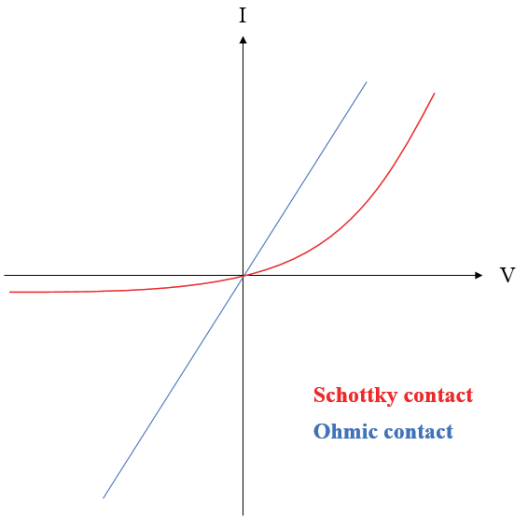

Fig. 3. (Color online) Schematic diagram of curves of ohmic and Schottky contacts.

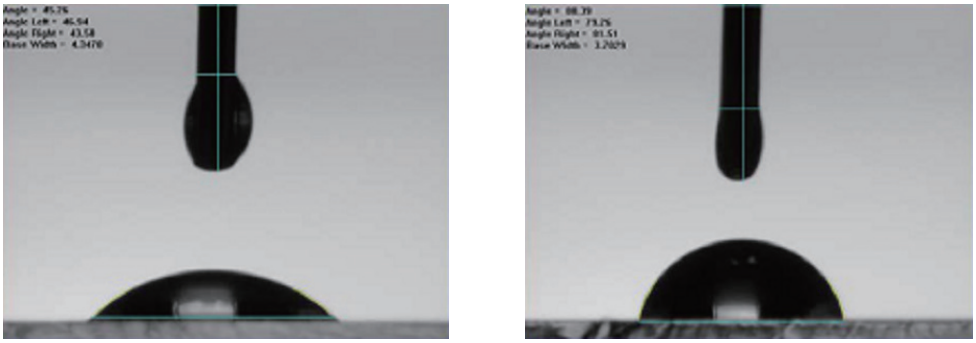

(a) (b)

Fig. 4. (Color online) Contact angles of (a) ITO glass and (b) untreated glass substrate.

The 2.5 mM chlorine doping resulted in more orderly and denser nanorod growth on the ZnO nanorod than on undoped samples. The cross-sectional view revealed that the growth direction of the chlorine-doped ZnO nanorod remained vertical to the substrate with a column height of 9.8 μm. The ZnO nanorod doped with 5.0 mM chlorine was more upright, orderly, and dense than that doped with 2.5 mM chlorine. The cross-sectional view of the 5.0 mM chlorine-doped ZnO nanorod showed a dense structure with a column height of 10.4 μm. The 7.5 mM chlorine-doped ZnO nanorod showed a more upright, orderly, and dense top view than the 5 mM chlorine-doped one. The 7.5 mM chlorine-doped ZnO nanorod grew longer with a column height of 11.6 μm. The 10.0 mM chlorine-doped ZnO nanorod showed the densest structure with a column height of 12 μm.

At higher chlorine doping concentrations, the ZnO nanorods grew more densely, uniformly, and vertically. The arrangement became more orderly, and the width of the nanorods also increased. Higher chlorine doping concentrations also led to a more uniform vertical growth

with increasing nanorod height. The results of energy-dispersive X-ray analysis (EDS) are shown in Fig. 5. The ratio of the weight of chlorine increased with the doping concentration. The EDS results of pure ZnO nanorods [Fig. 5(a)] and mass ratios of 0.24% (2.5 mM chlorine, not shown), 0.27% [5 mM chlorine, Fig. 5(b)], 0.31% (7.5 mM chlorine, not shown here), and 0.79% [10 mM chlorine, Fig. 5(c)] were obtained. The EDS results suggest that chlorine was successfully doped into the ZnO nanorods. Furthermore, the elemental distribution map confirmed the presence and distribution of chlorine in the ZnO nanorod.

The pure ZnO nanorods grown on the ZnO seed or SAMM layer and chlorine-doped ZnO nanorods at different concentrations were evaluated for power generation efficiency. The generation area was 1.5 × 1.5 cm^2. Electrical characteristics were measured using a precision digital multimeter (Keithley 2400) and an ultrasonic cleaner (42K Hz). The cleaner was operated in a 5 s on-and-off cycle for 1 min.

Figure 6 presents the power generation characteristics of the pure ZnO nanorod on the seed layer. The *I–V* curve shows good Schottky contact with a current ranging from −16.73 to 18.8 mA and a voltage from −3 to +3 V [(Fig. 6(a)]. The average current measured at zero voltage was 0.18 μA [Fig. 6(b)]. The average voltage measured at zero current was 4.41 mV [Fig. 6(c)]. The resulting average power was 0.77 nW. Figure 7 illustrates the power generation characteristics of the pure ZnO nanorod on a SAMM layer without a seed layer. The *I–V* curve indicates good Schottky contact with a current ranging from −23.9 to 25.16 mA and a voltage from −3 to +3 V [Fig. 7(a)]. The average current measured at zero voltage was 3.33 μA [Fig. 7(b)]. The average voltage measured at zero current was 16.76 mV with an average power of 55.73 nW [Fig. 7(b)].

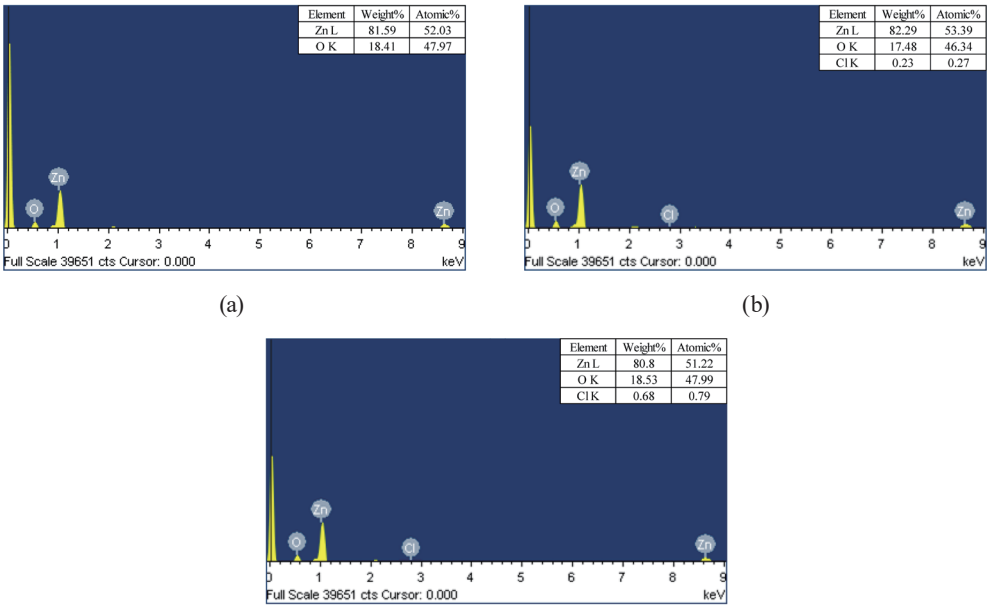

Fig. 5. (Color online) EDS elemental analysis results of (a) pure ZnO nanorods, (b) 5 mM chlorine-doped ZnO nanorod, and (c) 10 mM chlorine-doped ZnO nanorod.

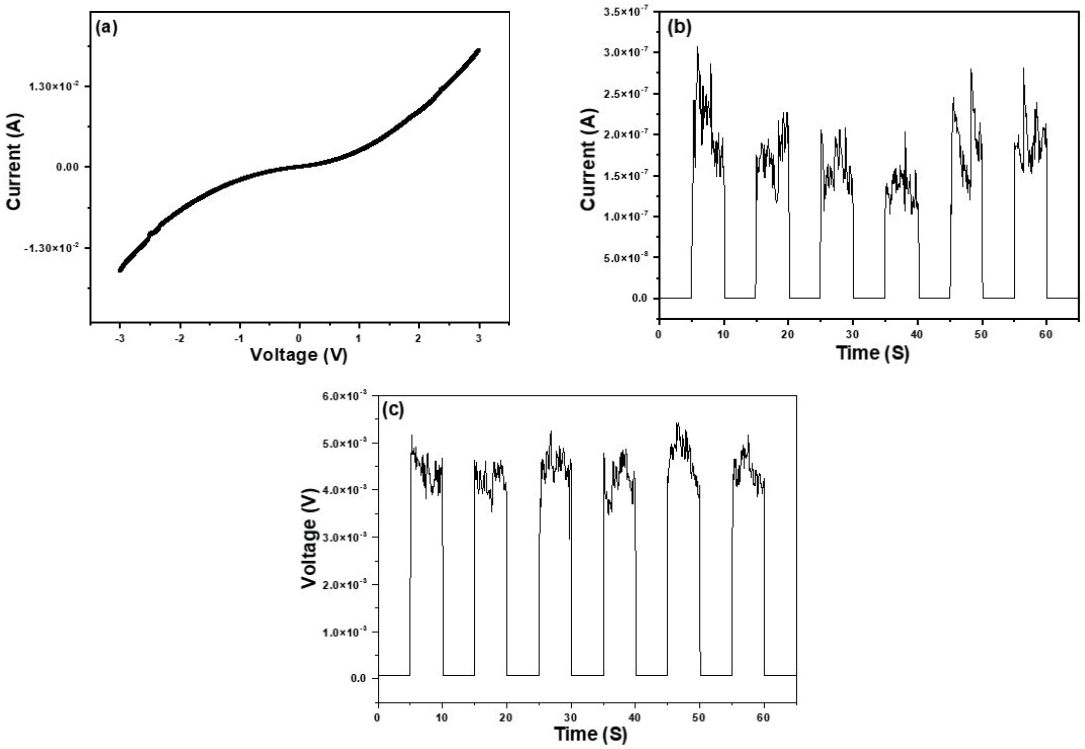

Fig. 6. Self-power-generation characteristics of ZnO nanorod grown on ZnO seed layer. (a) *I–V*, (b) average current, and (c) average voltage curves.

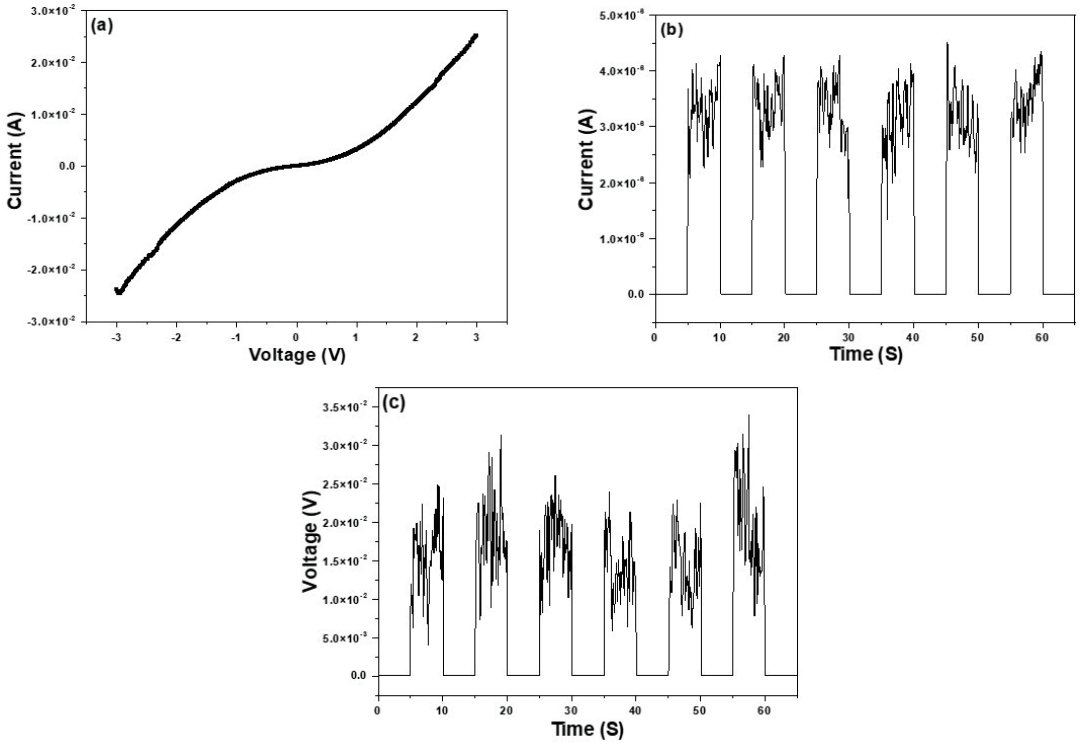

Fig. 7. Self-power-generation characteristics of pure ZnO nanorod grown on SAMM layer. (a) *I–V*, (b) average current, and (c) average voltage curves.

The *I–V* curve of the 2.5 mM chlorine-doped ZnO nanorod indicates good Schottky contact, with a current ranging from −30.02 to 30.74 mA and a voltage from −3 to +3 V. The average current at zero voltage was 3.07 μA, the average voltage at zero current was 22.93 mV, and the resulting average power was 70.3 nW. Figure 8 shows the power generation characteristics of the 5 mM chlorine-doped ZnO nanorod. The *I–V* curve indicates good Schottky contact with a current ranging from −33 to 26.7 mA and a voltage from −3 to +3 V [Fig. 8(a)]. The average current measured at zero voltage was 4.01 μA [Fig. 8(a)]. The average voltage measured at zero current was 20.8 mV, resulting in an average power of 83.43 nW [Fig. 8(c)].

The 7.5 mM chlorine-doped ZnO nanorod showed good Schottky contact with a current ranging from −35.14 to 33.71 mA and a voltage from −3 to +3 V. At zero voltage, the average current measured was 3.25 μA, and at zero current, the average voltage measured was 39.22 mV, resulting in an average power of 127.28 nW. The 10 mM chlorine-doped ZnO nanorod also had good Schottky contact with a current ranging from −35.56 to 47.88 mA and a voltage from −3 to +3V [Fig. 9(a)]. The average current measured at zero voltage was 5.62 μA [Fig. 9(b)]. The average voltage measured at zero current was 41.75 mV, resulting in an average power of 234.57 nW [Fig. 9(c)].

Table 1 shows that the average power obtained with a chlorine doping concentration of 10 mM was the highest, surpassing that of pure ZnO. The *I–V* curve for the 10 mM chlorine-doped sample also demonstrated the highest stability, with the Schottky curve being the most

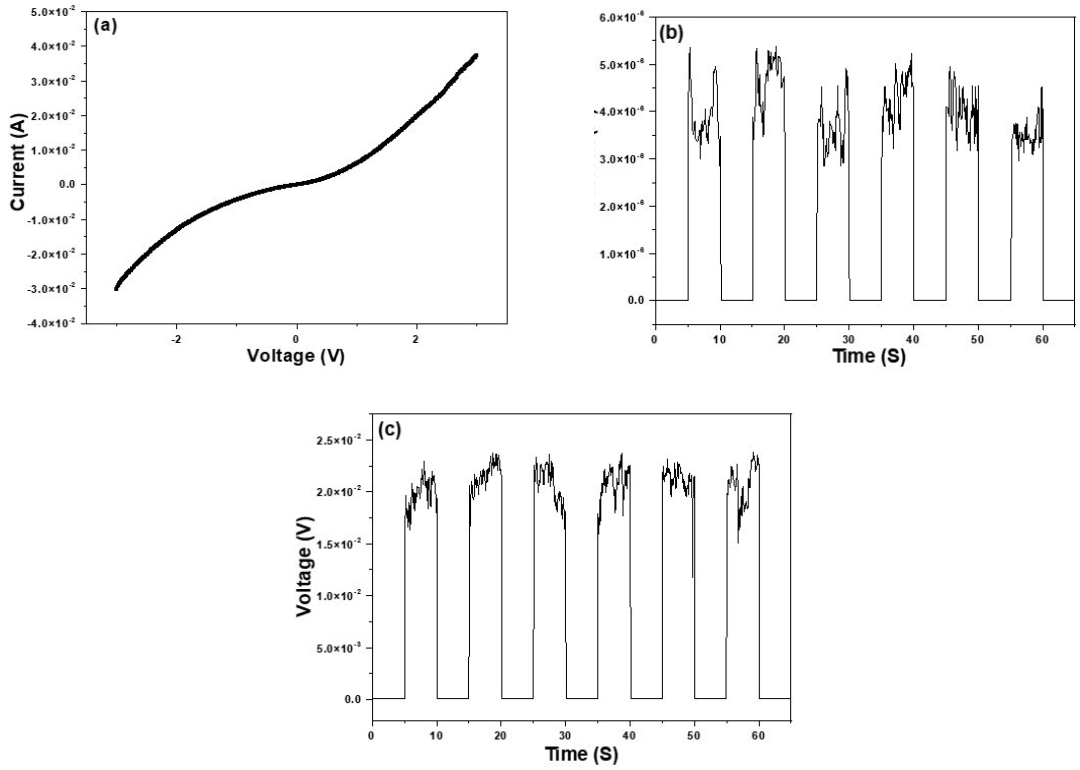

Fig. 8. Self-power-generation characteristics of 5 mM chlorine-doped ZnO nanorod grown on SAMM layer. (a) *I–V*, (b) average current, and (c) average voltage curves.

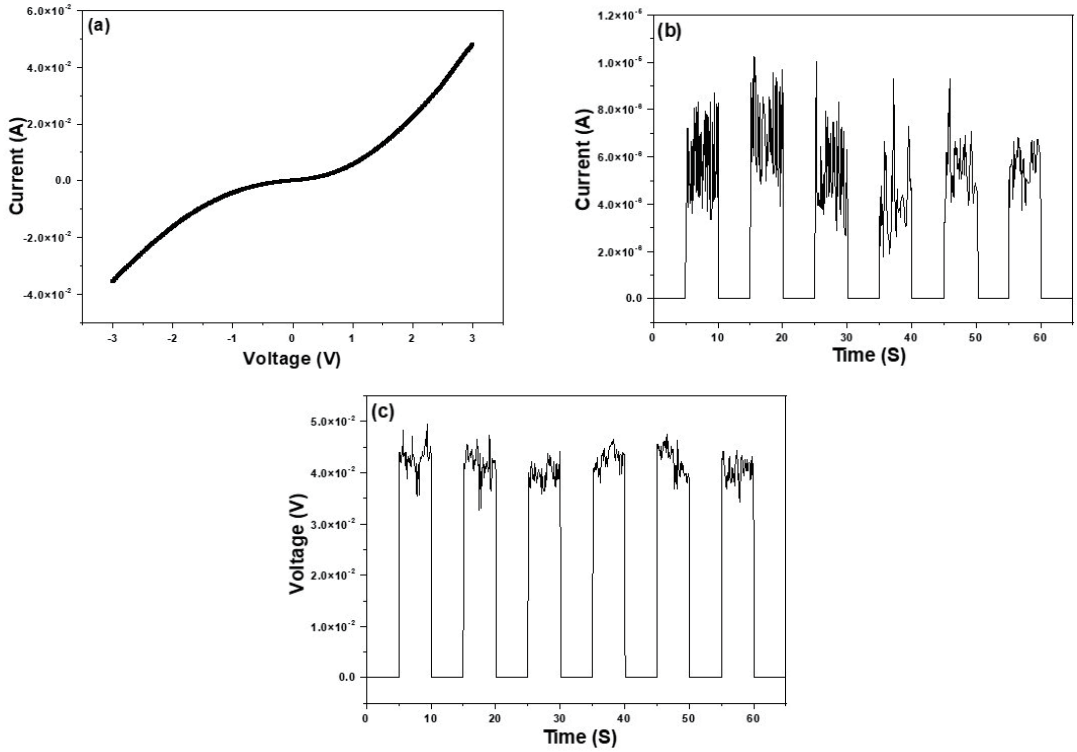

Fig. 9. Self-power-generation characteristics of 10 mM chlorine-doped ZnO nanorod grown on SAMM layer. (a) *I–V*, (b) average current, (c) average voltage curves.

Table 1
Characteristics of ZnO nanorods as nanogenerators, formed under different fabrication parameters.

Parameters	Average *I* (μA)	Average *V* (mV)	Average *P* (nW)	Power growth multiple
ZnO seed	0.18	4.41	0.77	1
SAMM	3.33	16.76	55.73	72.4
Doping 2.5 mM on SAMM	3.07	22.93	70.30	91.3
Doping 5 mM on SAMM	4.01	20.80	83.43	108.4
Doping 7.5 mM on SAMM	3.25	39.22	127.28	165.3
Doping 10 mM on SAMM	5.62	41.75	234.57	304.6

symmetrical. The ZnO nanorod grown on the SAMM layer exhibited higher piezoelectric characteristics than those on ITO. As the chlorine concentration increased, the power generation of the ZnO nanorods significantly increased. Using chlorine as a dopant enhanced the piezoelectric effect of ZnO nanorods. The highest enhancement was observed for the 10 mM chlorine-dopped ZnO nanorod, where the power generation efficiency increased to 304.6 times higher than that of the pure ZnO nanorod grown on ITO.

4. Conclusions

In this study, a piezoelectric nanogenerator was successfully fabricated by doping chlorine into the ZnO nanorods and growing them on the ZnO seed or SAMM layer. Chlorine was doped

at four different concentrations and the performance parameters of the ZnO nanorods doped with different Cl concentrations were measured and compared. After the thermal vapor deposition of the SAMM layer, the contact angle changed from 46.58 to 81.71°. The FE-SEM images showed that the ZnO nanorod grew more densely, uniformly, and vertically at higher chlorine concentrations. The EDS analysis results showed that the mass ratio of chlorine increased with the doping concentration. The mass ratios were 0, 0.24, 0.27, 0.31, and 0.78% for the pure ZnO nanorod and ZnO nanorods with chlorine doping concentrations of 2.5, 5, 7.5, and 10 mM, respectively. The average power of the fabricated piezoelectric nanogenerators was determined to be 55.73, 70.30, 83.43, 127.28, and 234.57 nW at the respective doping concentrations. The higher the doping concentration of chlorine, the more power was generated. Using chlorine as a dopant for ZnO nanorods markedly enhanced their piezoelectric effect. The most significant enhancement was observed with the ZnO nanorod doped with 10 mM chlorine, which achieved a power generation efficiency 304.6 times higher than that of the pure ZnO nanorod on ITO. This substantial increase underscores the potential of chlorine doping in enhancing the performance of ZnO nanorod nanogenerators.

References

1 S. Bairagi, S. Ghosh, and S. W. Ali: Sci. Rep. **10** (2020) 12121. https://doi.org/10.1038/s41598-020-68751-3
2 W. Deng, Y. Zhou, A. Libanori, G. Chen, W. Yang, and J. Chen: Chem. Soc. Rev. **51** (2022) 3380. https://doi.org/10.1039/d1cs00858g
3 W.-G. Kim, D. W. Kim, I.-W. Tcho, J.-K. Kim, M.-S. Kim, and Y.-K. Choi: ACS Nano **15** (2021) 258. https://doi.org/10.1021/acsnano.0c09803
4 S. N. Alam, A. Ghosh, P. Shrivastava, U. Shukla, K. Garg, A. C. Edara, and N. Sahoo: Nano-Struct. Nano-Objects **34** (2023) 100980. https://doi.org/10.1016/j.nanoso.2023.100980
5 M. A. Parvez Mahmud, A. Zolfagharian, S. Gharaie, A. Kaynak, S. H. Farjana, A. V. Ellis, J. Chen, and A. Z. Kouzani: Adv. Energy Sustainability Res. **2** (2021) 2000045. https://doi.org/10.1002/aesr.202000045
6 J. Briscoe and S. Dunn: Nano Energy **14** (2015) 15. https://doi.org/10.1016/j.nanoen.2014.11.059
7 Q. Xu, J. Wen, and Y. Qin: Nano Energy **86** (2021) 106080. https://doi.org/10.1016/j.nanoen.2021.106080
8 M. Ding, Z, Guo, L. Zhou, X. Fang, L. Zhang, L. Zeng, L. Xie, and H. Zhao: Crystals **8** (2018) 223. https://doi.org/10.3390/cryst8050223
9 S. Raha and Md. Ahmaruzzaman: Nanoscale Adv. **4** (2022) 1868. https://doi.org/10.1039/D1NA00880C
10 H. He, W. Cai, Y. Lin, and B. Chen: Langmuir **26** (2010) 8925. https://pubs.acs.org/doi/10.1021/la904723a
11 H. J. Fan, W. Lee, R. Hauschild, M. Alexe, G. Le Rhun, R. Scholz, A. Dadgar, K. Nielsch, H. Kalt, A. Krost, M. Zacharias, and U. Gçsele: Small **2** (2006) 561. https://doi.org/10.1002/smll.200500331